Fonseca, J., Bésuelle, P. & Viggiani, G. (2013). Micromechanisms of inelastic deformation in sandstones: An insight using x-ray micro-tomography. Geotechnique Letters, 3, pp. 78-83. doi: 10.1680/geolett.13.034

Fonseca, J., Bésuelle, P. and Viggiani, G. (2013) ***Géotechnique Letters*** **3**, No. 2, 78–83, http://dx.doi.org/10.1680/geolett.13.034

Micromechanisms of inelastic deformation in sandstones: an insight using x-ray micro-tomography

J. FONSECA*, P. BÉSUELLE† and G. VIGGIANI†

This study investigates the grain-scale mechanisms that lead to failure by strain localisation in specimens of Fontainebleau sandstone with different degrees of cementation. While the effects of inter-particle bonding on the mechanical behaviour of granular geomaterials, including soft rocks, have been largely studied, the physical micro-scale mechanisms governing the material deformation are still poorly understood. In this study, laboratory techniques have been developed to allow a non-invasive investigation of the internal deformation of sandstones during triaxial compression to failure. The material investigated was Fontainebleau sandstone, a quartzite formation from the Paris basin (France), which can be found as very hard, tightly cemented sandstone or more porous and less cemented material. Specimens with porosities of 6 and 21% were investigated. Triaxial compression tests at confining pressures of 2 and 7 MPa were conducted on dry cylindrical specimens of 11 mm diameter and 22 mm height. Three-dimensional (3D) images of the full specimens were obtained by carrying out x-ray micro-tomography scans at key points throughout the test. The high-resolution 3D tomographic images have a voxel size of 8·5 μm ($0{\cdot}033d_{50}$), allowing clear identification of the grains. This analysis suggests that dilatancy of the material, which depends on the degree of bonding between grains, plays a fundamental role in the failure mode of granular media. Insights into bonding rupture mechanisms and grain damage by inter- and intra-granular cracking are presented.

KEYWORDS: fabric/structure of soils; laboratory tests; particle crushing/crushability; particle-size behaviour; soft rocks; strain localisation

INTRODUCTION

Predicting the occurrence of failure in cohesive geomaterials by strain localisation is a key aspect in many geotechnical applications such as drilling technology, nuclear waste disposal and sequestration of carbon dioxide. Previous studies have shown that the failure mechanisms in porous soft rocks are highly dependent on the stress level (e.g. Wong *et al.*, 1997; Bésuelle *et al.*, 2000; Sulem & Ouffroukh, 2006; Charalampidou *et al.*, 2010). Bands of localised deformation have mechanical and structural evolutions that distinguish them from fractures and slip surfaces. The formation and evolution of a band of localised deformation involves a significant amount of grain rotation and translation, and can include grain crushing or merely rotation and frictional sliding along grain boundaries. These processes require a certain amount of porosity; if porosity is very low, then tension fractures and/or slip surfaces will preferentially form (Fossen *et al.*, 2007). Furthermore, in the case of permeability reduction, bands of localised deformation could act as barriers to fluid flow in otherwise more permeable rock, impacting extraction and storage of fluids (e.g. Issen & Rudnicki, 2000). This study investigates the deformation of sandstones with different degrees of cementation tested in triaxial compression at different confining pressures and the micro-scale mechanisms associated with the macroscopic behaviour.

Manuscript received 21 March 2013; first decision 14 April 2013; accepted 1 May 2013.
*City University London, London, UK
†Grenoble-INP, UJF-Grenoble 1, CNRS UMR 5521, Laboratoire 3SR, Grenoble, France

EXPERIMENTAL METHOD

Material description

The material investigated was Fontainebleau sandstone from the Paris basin in France. Fontainebleau is a pure quartz sandstone (approximately 100% quartz) of Oligocene age (Stampian); it is a well-sorted material with a median grain size of 260 μm. An outstanding feature of this formation is the contrast between the very hard, tightly cemented sandstone and the more porous and less cemented material. In its intact state, this rock can be found in a wide range of porosities varying from 2 to 30% without noticeable grain size modification (Bourbie & Zinszner, 1985). Silicification processes occurring after deposition of Fontainebleau sands have developed grain cementation by quartz overgrowths (Grisoni & Thiry, 1988; Thiry *et al.*, 1988). Subangular grains with some very angular facets, rare grain inter-penetrations and an absence of matrix material characterise this shallowly buried sandstone (Thiry & Marechal, 2001).

Specimens from two different locations and with porosities of 6 and 21% were studied. This difference in porosity and the degree of cementation results in two very distinct microstructures, as illustrated in Figs 1(a) and 1(b). Figure 1(a) shows a section through an x-ray tomographic volume (acquired at a resolution 6·5 μm) for the material with approximately 6% porosity (referred to as 'stiff sandstone' hereafter). This material exhibits a very dense packing with abundant subhedral overgrowths that developed during sandstone cementation. Polygonal contacts, rectilinear and often convergent to triple junctions, can be observed. The microstructure of the 'soft sandstone' (approximately 21% porosity) is shown in Fig. 1(b). This lightly cemented material nonetheless exhibits a dense packing with extensive contacts between grains. These microstructural characteristics are often associated with a

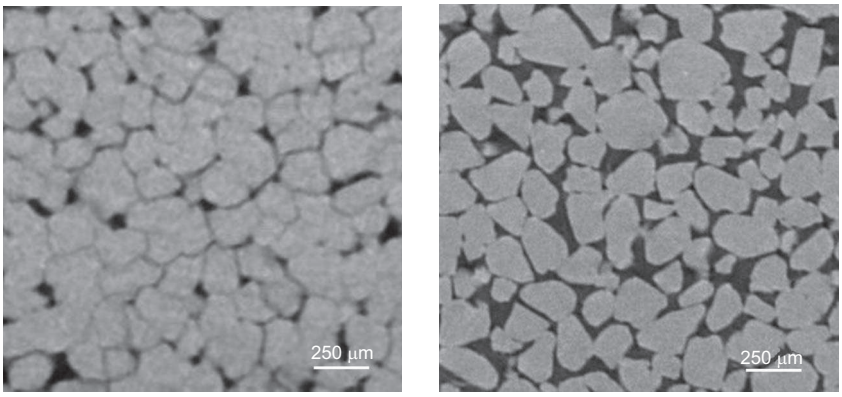

Fig. 1. Sections through x-ray tomographic 3D images of Fontainebleau sandstone with approximately (a) 6% porosity and (b) 21% porosity

locked structure (Dusseault & Morgenstern, 1979). The topology of this sandstone presents large similarities with Reigate sand from south-east England, a locked sand with virtually no bonding between grains and in which the strong fabric plays a fundamental role in the behaviour of the intact material (Fonseca *et al.*, 2012). Fontainebleau is not likely to fit into the locked material classification; it is a geologically recent formation and does not appear to exhibit inter-penetrative or sutured contacts induced by pressure solution. The subangular particle shape and the existence of grains with flat sides allow the formation of extensive contacts, which could have an impact on the shear stiffness and peak strength of the material (Fonseca *et al.*, 2013a).

Triaxial tests

Specimens were cored from large blocks retrieved from the site to approximately 11 mm diameter; the length of the cylindrical cores was reduced to approximately 22 mm using coarse sandpaper. The ends of the cylinders were smoothed using a very thin layer of epoxy resin (approximately 0·4 mm thick, i.e. $1{\cdot}6d_{50}$). This resin layer allowed smoothing of the ends of the samples, avoided leakage due to possible damage of the membrane during testing and was helpful in obtaining flat and parallel ends. The technique was particularly useful for the stiff material given the difficulty in obtaining flat ends by grain plucking as the grains tended to be removed in small clusters rather than individual grains when using sandpaper to reduce the cylinder height.

Triaxial compression tests were carried out on dry specimens following isotropic compression at pressures of 2 and 7 MPa. The tests were performed in a small high-pressure triaxial cell specifically designed to operate inside the x-ray scanner, allowing in situ scans to be carried out (in situ meaning x-ray scanning at the same time as loading). Deviatoric loading was applied by an ascending piston at a rate of 21 μm/min (approximately 0·1%/min). Between five and seven loading stages were imaged during each test, as shown in Fig. 2. The scans were taken at a spatial resolution of 8·5 μm, meaning that the diameter of a median size grain was represented by approximately 30 voxels.

Figure 2 shows the mechanical response for all the soft and stiff specimens. The loading stages chosen for imaging are marked by small axial stress relaxations, taking place in a few minutes when loading was stopped in order to perform an x-ray scan. The time required to scan the top and bottom of the specimen was approximately 4 h (due to detector size limitations, the top and bottom parts of the sample were scanned separately and stitched together to obtain the full specimen). For the soft material (Fig. 2(a)), two samples were tested at 7 MPa and two samples at 2 MPa. The four specimens exhibited brittle behaviour when subjected to an increase in deviatoric stress, with the specimens tested at 7 MPa showing higher peak and residual stresses. For the specimens tested at 2 MPa, the difference in the stress–strain response can be explained by the confining pressure oscillations (maximum value of 500 kPa) during test FBS04-2MPa. All the specimens had end lubrication with the exception of sample FBS01-7MPa. Figure 2(b) shows the behaviour of the three stiff specimens tested at 2 MPa (higher pressures were not possible due to the axial force transducer limitation of 10 kN). The material showed brittle behaviour up to peak stress, followed by an abrupt drop to a residual stress.

OBSERVATIONS

The different patterns of failure obtained for the soft sandstone are shown in Fig. 3. The cross-sections (perpendicular to the axis of the specimen) and vertical sections taken at load stage 1 for sample FBS03-2MPa (Fig. 3(a)) and at the last load stage for samples FBS03-2MPa (Fig. 3(b)), FBS04-2MPa (Fig. 3(c)) and FBS02-7MPa (Fig. 3(d)) are shown in the figure. Specimens FBS03-2MPa and FBS02-7MPa failed along a well-defined shear band with an orientation angle with respect to the minor principal stress (the horizontal direction) of 53° and 48° for the tests at 2 and 7 MPa, respectively. The slight isotropic unloading of test FBS04-2MPa is likely to have caused the unbonding of grains (Alvarado *et al.*, 2012). Once unbonded, the grains are less restrained to rearrange, which leads to higher dilation and less localised deformation and the development of multiple and diffuse shear planes. The shear zone can be identified as a region of intense grain breakage and slightly larger pores for sample FBS03-2MPa while, for the 7 MPa samples, grain fragments and crushed material fill the pore space. In both cases the thickness of the band of localised deformation is approximately $4d_{50}$ to $6d_{50}$ (i.e. 1·0–1·5 mm).

The tightly cemented material (stiff sandstone) exhibited a more complex failure mode. No apparent change in microstructure was observed until a small plateau (shown in detail in Fig. 2(b)) was observed in the stress–strain curve; this marked the initiation of axial splitting and occurred in the three samples shortly after 2% of axial

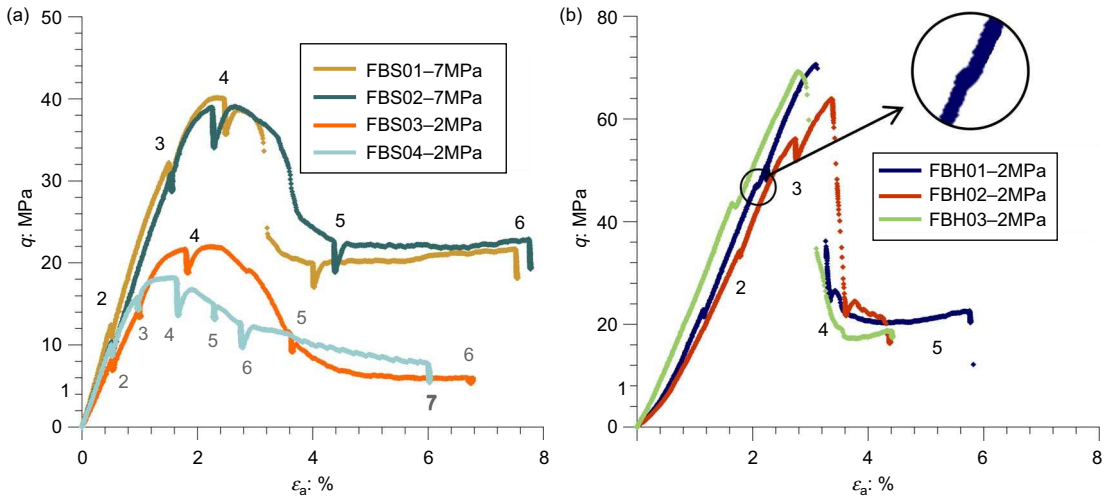

Fig. 2. Deviatoric stress (q) against global axial strain (ε_a) for the specimens tested with indication of the loading stages chosen for imaging (marked by small relaxations in the stress deviator) for (a) soft sandstone and (b) stiff sandstone (note different vertical scales used in the plots)

shortening. This was followed by a further increase in deviatoric stress while vertical cracks in the sample expanded up to the point where the sample collapsed and the stress dropped dramatically to a residual value. This coincided with the development of multiple dilatant shear planes, which appeared to increase in thickness with further deformation. Figure 4 shows the deformation of the material from load stage 2 to load stage 5. Two types of deformation bands were observed: open vertical fractures with an aperture of 0·7 mm and shear bands up to 2·5 mm thick and with intense grain crushing, similar to those observed in the soft material at 7 MPa.

DISCUSSION

Evolution of the microstructure and the mechanisms that led to failure of the specimens are discussed in this section. Changes in the fabric of the soft sandstone due to strain localisation were not observed until the post-peak regime, as also reported in previous studies (Menéndez *et al.*, 1996; Sulem & Ouffroukh, 2006). Microstructural changes in the strain hardening regime are below image resolution but are believed to be related to elastic deformation of the skeleton, grain rearrangement and inter-granular cracking from grain to grain. Despite the shear rupture of lithified and cemented grain contacts in localised regions, the grains cannot rearrange unless there is a reduction in stress that allows the restrained grains to translate and/or rotate. This hypothesis is supported by the less localised deformation observed in specimen FBS04-2MPa, which experienced a slight decrease in confining pressure through shearing (Fonseca *et al.*, 2013b). Intra-granular cracking was observed at peak, although micro-cracks (below image resolution) could possibly start forming earlier. Higher resolution (6·5 μm) images of Fontainebleau sandstone prior to loading did not show signs of pre-existing cracks, as would be expected for this shallow buried sandstone, which was unlikely to have experienced large inter-particle stresses during the diagenesis process. The propagation of intra-granular cracking leads to disintegration of the grains

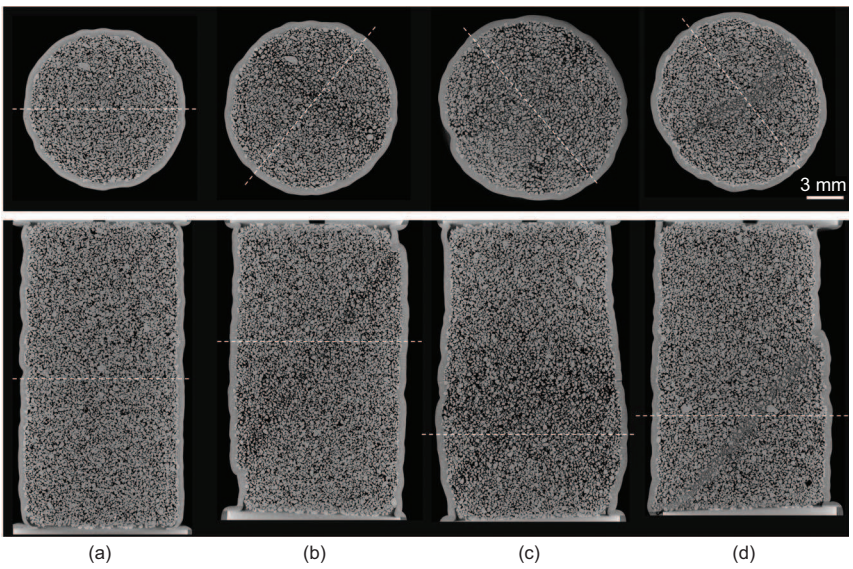

Fig. 3. Cross-sections (upper) and vertical sections (lower) for (a) sample FBS03-2MPa at load stage 1, (b) sample FBS03-2MPa at load stage 6, (c) sample FBS04-2MPa at load stage 7 and (d) sample FBS02-7MPa at load stage 6 (location of the sections indicated by the dashed lines)

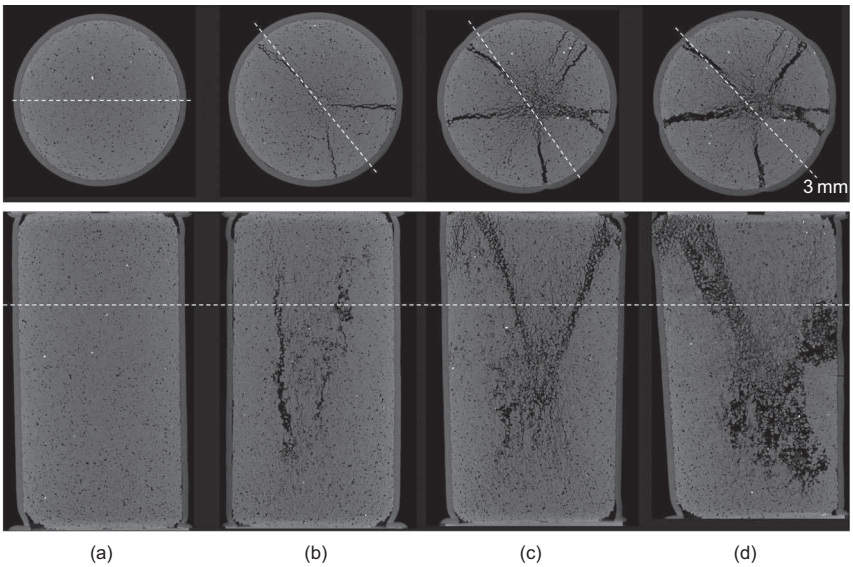

Fig. 4. Cross-sections (upper) and vertical sections (lower) for sample FBH01-2MPa at (a) load stage 2, (b) load stage 3, (c) load stage 4 and (d) load stage 5 (location of the sections indicated by the dashed lines)

into small fragments, loss of stability in the primary fabric of the stress transmission particles and consequent strain softening of the specimen. This creates local degrees of freedom that allow grains to translate and rotate. The shear band is a result of these mechanisms.

Intra-granular cracking is not restricted to the shear band but was seen to occur throughout the specimen, being more intense at higher confining pressure. Local stress concentration induces the initiation of these cracks, which appear to initiate at grain contact and show an orientation close to the vertical direction, i.e. parallel to the orientation of the major stress (Fig. 5(a)). The nature of the contact has a primary influence on the initiation of intra-grain cracking and therefore in the overall deformation of the material. As shown in Fig. 5(b), extended contacts between grains are more likely to inhibit cracking than point-like contacts. Together with the orientation (with respect to the direction of the major principal stress) and the size of the contact, the coordination number and the size of the particles in contact have a major influence on the damage mechanisms occurring on a grain or a group of neighbouring grains. The cushioning effect on large grains surrounded by small ones has been reported in previous studies (e.g. Tsoungui *et al.*, 1999). Figure 6 shows a large grain in contact with many small grains (contact L–S). High coordination numbers lead to a less heterogeneous distribution of the stresses inside the grain, making it less susceptible to crushing. In addition, a large grain in contact with many small ones is less restricted to rotate and consequently to lose contacts, as illustrated in Fig. 6(b). Being less restricted to move also prevents grain damage. Large grains can be damaged when in contact with other large particles (contact L–L), as shown in Fig. 7.

Interesting insights into the damaging of cement between grains can be gained from study of the deformation of the stiff sandstone. As illustrated in the vertical sections shown in Fig. 8, the cement breaks along vertical ridges, which leads to the formation of vertical columns of horizontally unbonded grains that are able to transfer stresses along the direction of the major principal stress direction. Conversely to the soft material, intra-granular cracking is inhibited by the cemented extended contact between the grains and is observed only in regions of localised deformation where the initial contacts have been lost. As shearing progresses, the vertical columns of grains transmitting forces (force chains) will eventually collapse and the unbonded grains increase the thickness of the shear band.

CONCLUSIONS

This study has shown how measuring deformation at the grain-scale during a test can significantly advance understanding of

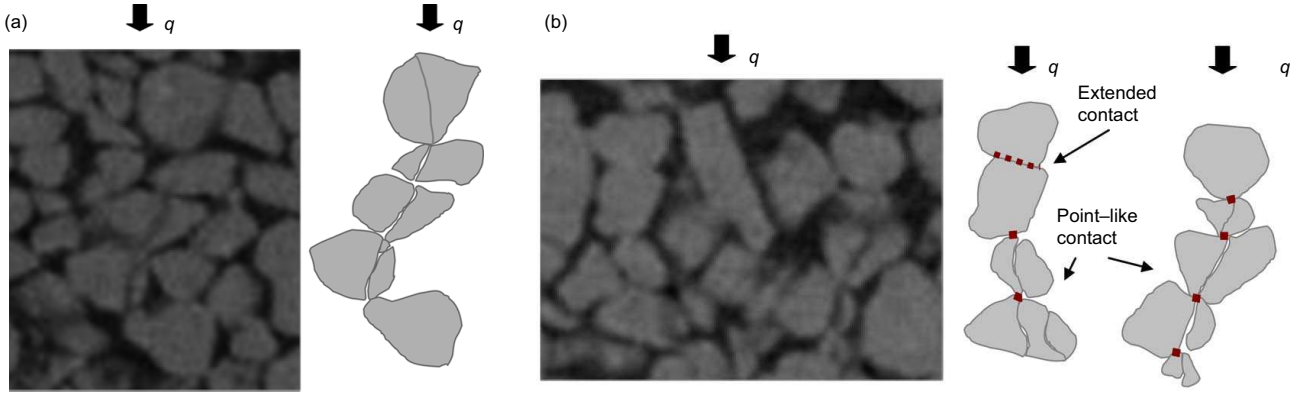

Fig. 5. Vertical sections from sample FBS03-2MPa (load stage 6) in a region above the shear band and schematic diagrams illustrating crack propagation in subvertical directions

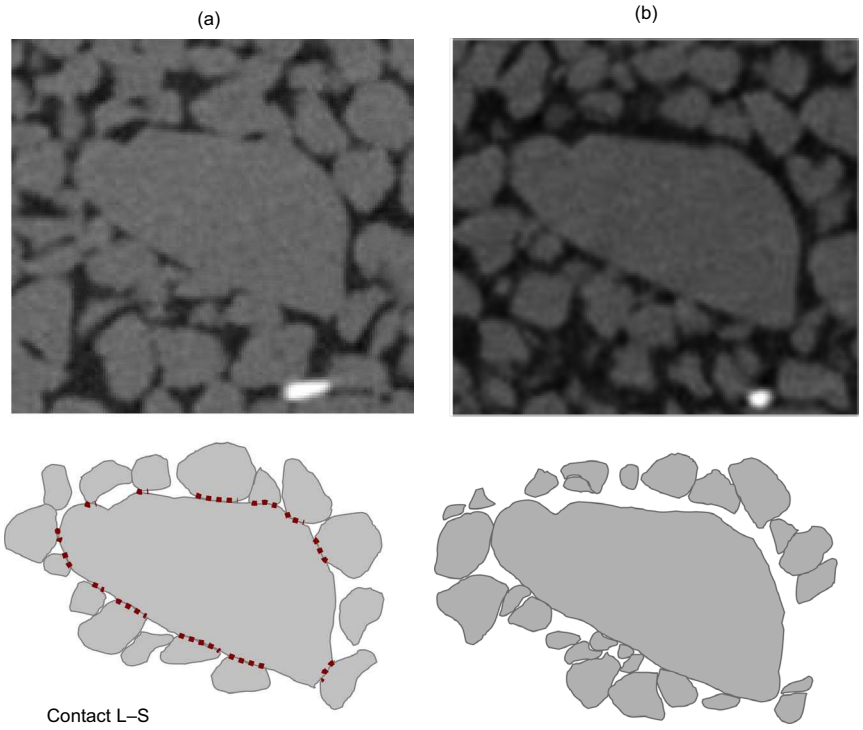

Fig. 6. Horizontal section from sample FBS03-2MPa and respective schematic diagram for (a) load stage 0 and (b) load stage 6

the micromechanisms responsible for the mechanical behaviour observed at the macro-scale. In particular, it has been shown that the nature of bonding strongly affects evolution of the microstructure with shearing and, consequently, the failure mode at the macro-scale. Axial splitting through the cement followed by the development of multiple shear bands was observed in the stiff sandstone, while the soft material failed along a well-defined shear plane.

Insights into the damage mechanisms of bonded granular materials and the evolution of their microstructure have been presented. It is suggested that dilatancy characteristics, which depend on the degree of bonding between grains, play a fundamental role in the failure mode of the material. The damage mechanism consisted, in both cases, of an initial rupture of the cement between grains, which was more severe for the stiff material, followed by intra-granular cracking, less common for the strongly bonded grains. The propagation of cracks and the initiation of grain breakage are believed to lead to a loss of stability in the primary fabric of the grains transmitting the stress and consequently to strain softening of the specimen. This creates local degrees of freedom that allow grains to translate and rotate. The examples shown in this study indicate that shear bands include both grain rotation and frictional sliding along grain boundaries, as well as breakage and crushing of grains. The relative incidence of each of these phenomena is controlled essentially by the loading conditions and nature of the contacts.

When modelling grain-scale phenomena such as strain localisation, experimental grain-scale observations such as those reported here are of utmost importance. The information provided by x-ray tomography (when combined with three-dimensional (3D) image analysis) is much more powerful than that obtained from scanning electron microscopy techniques for example, not only because it is 3D but also because it is not destructive and thus allows study of microstructure in a 'fourth dimension' – time or, in other words, deformation. This has successfully allowed characterisation of the micromechanisms underlying the deformation of unbonded granular materials (e.g. Andò *et al.*, 2012). However, the quantitative grain-scale study of

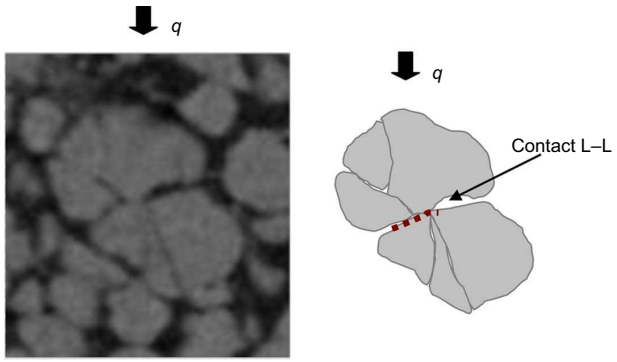

Fig. 7. Vertical section from sample FBS03-2MPa (load stage 6) from a region located at the boundary of the shear band and schematic diagram showing crack propagation for two large grains in contact

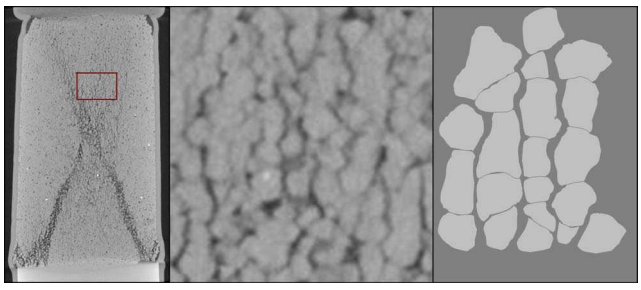

Fig. 8. Vertical sections of sample FBH02-2MPa at the last stage of loading (a), detailed view of the marked region (b) and schematic illustration (c)

bonded granular materials is considerably more challenging because grain-scale processes involve not only grain rearrangement, but also debonding and the production of fines by grain breakage. Further work is certainly needed and, although interesting and promising, the results reported in this paper are to be considered just preliminary steps in this direction.

Acknowledgement

This work was carried out within the framework of the project GEOBRIDGE funded by the French Research Agency ANR (contract number ANR-09-BLAN-0096).

REFERENCES

Alvarado, G., Coop, M. R. & Willson, S. M. (2012). On the role of bond breakage due to unloading in the behaviour of weak sandstones. *Géotechnique* **62**, No. 4, 303–316, http://dx.doi.org/10.1680/geot.8.P.017.

Andò, E., Hall, S. A., Viggiani, G., Desrues, J. & Bésuelle, P. (2012). Experimental micromechanics: grain-scale observation of sand deformation. *Géotech. Lett.* **2**, No. 3, 107–112.

Bésuelle, P., Desrues, J. & Raynaud, S. (2000). Experimental characterisation of the localisation phenomenon inside a Vosges sandstone in a triaxial cell. *Int. J. Rock Mech. Mining Sci.* **37**, No. 8, 1223–1237.

Bourbie, T. & Zinszner, B. (1985). Hydraulic and acoustic properties as a function of porosity in Fontainebleau sandstone. *J. Geophys. Res.* **90**, No. B13, 11524–11532.

Charalampidou, E. M., Hall, S. A., Stanchits, S., Lewis, H. & Viggiani, G. (2010). Characterization of shear and compaction bands in a porous sandstone deformed under triaxial compression. *Tectonophysics*, **503**, No. 1–2, 8–17.

Dusseault, M. B. & Morgenstern, N. R. (1979). Locked sands. *J. Engng Geol.* **12**, No. 2, 117–131.

Fonseca, J., O'Sullivan, C., Coop, M. R. & Lee, P. D. (2012). Quantifying the evolution of soil fabric during shearing using directional parameters. *Géotechnique* **63**, No. 6, 487–499, http://dx.doi.org/10.1680/geot.12.P.003.

Fonseca, J., O'Sullivan, C., Coop, M. R. & Lee, P. D. (2013a). Quantifying the evolution of soil fabric during shearing using scalar parameters. *Géotechnique* http://dx.doi.org/10.1680/geot.11.P.150.

Fonseca, J., Bésuelle, P. & Viggiani, G. (2013b). An experimental study of micro-scale deformation in a soft sandstone. *Proc. 1st Int. Conf. on Tomography of Materials and Structures*. In press.

Fossen, H., Schultz, R. A., Shipton, Z. K. & Mair, K. (2007). Deformation bands in sandstone: a review. *J. Geol. Soc.* **164**, No. 4, 755–769.

Grisoni, J. C. & Thiry, M. (1988). Répartition des grès dans les Sables de Fontainebleau. Implications géotechniques des études récentes. *Bull. Liaison Lab P. et Ch*. **157**, 17–28.

Issen, K. A. & Rudnicki, J. W. (2000). Conditions for compaction bands in porous rock. *J. Geophys. Res.* **105**, No. B9, 21529–21536.

Menéndez, B., Zhu, W. & Wong, T.-F. (1996). Micromechanics of brittle faulting and cataclastic flow in Berea sandstone. *J. Struct. Geol.* **18**, No. 1, 1–16.

Sulem, J. & Ouffroukh, H. (2006). Shear banding in drained and undrained triaxial tests on a saturated sandstone: porosity and permeability evolution. *Int. J. Rock Mech. Mining Sci.* **43**, No. 2, 292–310.

Thiry, M. & Marechal, B. (2001). Development of tightly cemented sandstone lenses in uncemented sand: example of the Fontainebleau sand (Oligocene) in the Paris basin. *J. Sediment. Res.* **71**, No. 3, 473–483.

Thiry, M., Bertrand-Ayrault, M. & Grisoni, J. C. (1988). Ground water silicification and leaching in sands: example of the Fontainebleau sand (Oligocene) in the Paris basin. *Geol. Soc. Am. Bull.* **100**, No. 8, 1283–1290.

Tsoungui, O., Vallet, D. & Charmet, J.-C. (1999). Numerical model of crushing of grains inside two-dimensional granular materials. *Powder Technol.* **105**, No. 1–3, 190–198.

Wong, T. F., David, C. & Zhu, W. (1997). The transition from brittle to cataclastic flow: mechanical deformation. *J. Geophys. Res.* **102**, No. B2, 3009–3025.